A penalized motion detection model for extracting ionospheric echoes from low signal-to-noise ratio Ionogram video images

Yuu Hiroshige
Department of Creative Informatics, Kyushu Institute of Technology, 680-4 Kawazu, Iizuka, 820-8502, Japan

Akiko Fujimoto
Department of Artificial Intelligence, Kyushu Institute of Technology, 680-4 Kawazu, Iizuka, 820-8502, Japan

Akihiro Ikeda
National Institute of Technology, Kagoshima College, 1460-1 Shinko, Hayato, Kirishima, Kagoshima, 899-5193, Japan

Shuji Abe
International Research Center for Space and Planetary Environmental Science, Kyushu University, 744, Motooka, Nishi-ku, Fukuoka, 819-0395, Japan

Akimasa Yoshikawa
International Research Center for Space and Planetary Environmental Science, Kyushu University, 744, Motooka, Nishi-ku, Fukuoka, 819-0395, Japan

Email: hiroshige.yuu147@mail.kyutech.jp, fujimoto@ai.kyutech.ac.jp, a-ikeda@kagoshima-ct.ac.jp, abeshu@i-spes.kyushu-u.ac.jp, yoshikawa.akimasa.254@m.kyushu-u.ac.jp
www.kyutech.ac.jp

Abstract

Measuring the altitude distribution of electron density in the upper atmosphere, known as the ionosphere, using High-Frequency radio wave reflections often causes the low signal-to-noise ratio of ionospheric echoes due to radio frequency interference. We propose a model for converting low-signal-to-noise-ratio ionospheric echo video images (Ionogram) into noise-reduced images using image processing techniques, for tracing the ionospheric echoes from Ionogram. The proposed method consists of three processing parts: noise removal optimized for individual Ionogram images, extraction of ionospheric echoes by penalized background subtraction technique, and fine-tuning of ionospheric echo signals using a minimum spanning tree algorithm. The proposed model successfully reproduces fine Ionograms with 98% recall and 99% precision.

Keywords: Ionospheric Observation, Computer Vision, Motion Detection, Time-series data

1. Introduction

The ionosphere is a part of Earth's upper atmosphere from about 100km to high altitudes and is very closely related to our modern life. The ionosphere has a significant impact on the radio propagation for communications, satellite positioning system, etc. The structure of ionosphere is not stable and variable in the time of day, season, latitude, and solar activity, because of the differences of the energetic photo-ionization process. The irregularities and disturbances in the ionosphere cause various severe problems, for example, lower accuracy of the radio navigation due to the global positioning system/Global Navigation Satellite System scintillation, disruptions in High Frequency (HF) radio wave bands or interferences due to anomalous propagation, etc. In order to utilize radio propagation safely and securely in modern society, it is essential to measure and analyze the fluctuating ionospheric environment at high speed and with high accuracy.

The fluctuating ionospheric environment is characterized by electron density variations in this region. The fluctuating ionospheric environment is characterized by electron density variations in this region. Ionosonde, a vertical ionospheric sounder, has been widely used to detect the ionospheric electron density as a function of height, using HF radio wave reflections. Ionosonde emits radio impulses with increasing frequency, measuring the time delay of radio signals received back from the different ionospheric layers. Fig. 1a shows an ionogram, which is a visualization of the output of an ionosonde measurement. The ionogram represents the received echo intensities in a virtual height (time-of-flight) against transmitted frequency. To analyze the fluctuating ionospheric environment, it is important of the interpretation of the ionogram, the so-called "scaling" of

ionograms. In other words, the scaling is the detection of the ionospheric echo on the ionograms and the extraction of characteristics of E and F layers (virtual heights: h'E, h'F, h'F2, etc. or critical frequencies: foE, foF1, foF2, etc.) from ionograms [1].

Classical manual scaling by professional researchers has been used, but several methods of automatic scaling have been proposed in recent decades. There are two main approaches to automatic scaling: image processing (computer vision) approaches [2], [3] and deep-learning image generation approaches [4], [5]. The both methods perform the scaling of ionograms with higher accuracy, but the expected ionogram for scaling is high signal-to-noise ratio (SNR) image. Here, the signal is the ionospheric echo, and the noise is the background noise, such as radio frequency interference (RFI) from other emissions. In Fig. 1a, the noise appears as the vertical strip. The ionogram visualization process also generates noise [6]. Ionogram images are visualized using spectral analysis techniques such as the Fast Fourier Transform (FFT) algorithms on original data obtained by the ionosonde. Artificial noises are generated by this process. The noise due to RFI and FFT complicates automatic information extraction from ionogram through scaling [7].

Ionosonde transmitting power by a typical HF radar is high power, several tens of kW. In ionogram images acquired by such high-power ionosondes, the signal strength of the ionospheric echo and the background noise are distinctly different, and the ionospheric echo is sufficiently strong. This means that scaling can be performed from ionogram images with high SNR. On the other hand, our ionosonde observations with Frequency Modulated Continuous Wave (FM-CW) type radar, operated by the joint research with Kyushu Institute of Technology and Kyushu University, have a maximum peak power of 20 watts. Although the advantage of FM-CW radar is its high gain even at low power, the reflected echo strength from the ionosphere is relatively weak compared to a typical HF radar. Therefore, the signal strength of the ionospheric echoes is often comparable to the background noise, and it is difficult to separate from each other. Since the scaling process is performed from ionogram images with low SNR, a simple noise elimination processing is not sufficient.

There are two challenges in automatic ionogram scaling for FM-CW ionogram. First, as described above, scaling accuracy is poor when the input image is an ionogram with low SNR. Second, in terms of the quasi-real-time monitoring of the ionospheric condition, the processing time on scaling is required within few seconds. We sequentially operate the FM-CW ionosonde with every 3 minutes. A low-cost computer, which is usually expected to perform with no high processing speed, is required on the observation site. The deep learning approaches have a processing time of 2-3 minutes, and real-time scaling requires a computer with high processing speed. We try to propose a new algorithm without deep-learning approach for scaling which includes the elimination process of background noises.

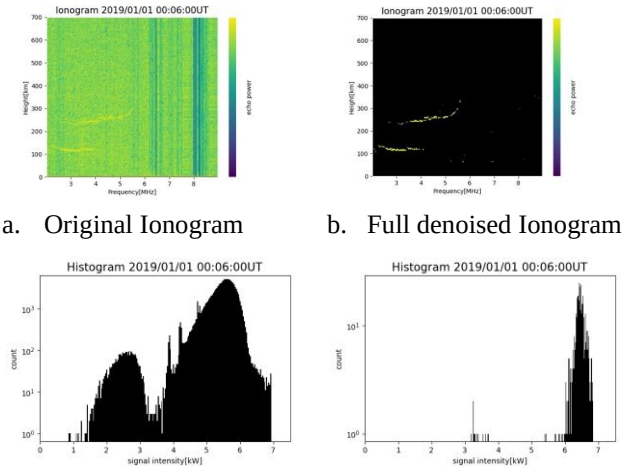

a. Original Ionogram b. Full denoised Ionogram

c. Histogram of signal intensity for Fig .1a d. Histogram for signal intensity of Fig. 1b

Fig. 1. Comparison of the signal intensities of original and full denoised ionograms recorded at 00:06:00 UT, January 1, 2019.

In this paper, we provide a new method to scaling of FM-CW ionogram with low SNR. The new scaling method can be applied to ionograms containing any ionospheric echo class (E and F layers) for quasi-real-time detection. The shape and position of the ionogram echoes vary with time, due to daily and seasonal changes in the ionospheric electron density structure and its solar activity dependence. Therefore, our study focuses on time-variant scaling based on time-series analysis. The proposed method consists of three parts. First, we remove the noise from the ionogram with low SNR, optimizing the noise elimination threshold value for individual ionogram image. Second, we extract the ionospheric echoes based-on penalized background subtraction technique. Finally, the ionogram with high SNR are regenerated by fine-tuning of ionospheric echo signals using a minimum spanning tree algorithm.

2. Dataset

The dataset used in this study consists of 960 ionogram data observed every 90 seconds on January 1, 2019, at the FM-CW radar ionosonde located at Sasaguri (130.34° E, 33.37° N). Fig. 1a shows a sample of the ionogram image data obtained on January 1, 2019, at 00:06:00 UT (Universal Time). Ionogram image shows the signals with frequency values from 2 MHz to 9 MHz and altitude values from 0 km to 700 km. In order to treat the ionograms as a two-dimensional array, we consider the class width as an array with 278 x 238 bins with a frequency of 0.25 MHz and an altitude of 2.9296875 km.

As mentioned above, the ionogram is usually contaminated with RFI noise appearing as vertical strips,

shown in Fig. 1a. As shown in Fig. 1, the signal intensity distribution in histograms is significantly different between the original ionogram (Fig. 1c) and the full denoised ionogram (Fig. 1d). Fig. 1b was produced by manual removal of the background noise from Fig. 1a. The signal distribution in Fig. 1d only corresponds to the ionospheric echoes. Comparing between Fig. 1c and Fig. 1d, it is obvious that ionospheric echoes are highly intense relative to noises. In other words, the almost background noises are in lower value of signal intensity.

3. Methodology

The proposed method consists of three processing parts: (1) Weak Signal Reduction, (2) Penalized Background Subtraction, and (3) Fine-tuning Ionogram. In the processing part on Weak Signal Reduction, the divided value between the ionospheric echoes and the background noises is automatically estimated based-on Ridge Regression [8]. After this process, almost background noises are eliminated, and we get the denoised ionogram remaining enough ionospheric echoes. The processing part of Penalized Background Subtraction enables the extraction of ionospheric echoes with motion detection algorithms. Finally, the processing part of Fine-tuning Ionogram provides the regenerated ionogram, removing the remained noises and interpolating the ionospheric echoes from the detection region using the minimum spanning tree in the graph structure. The following subsections describe the detail algorithm of each part.

3.1. *Weak Signal Reduction*

As pre-processing, the weaker RFI noises are eliminated by aligning the average signal strength in the altitude direction to a constant value, which is the mode of histogram of signal intensity. We define the elimination function of RFI noises as below:

$$\boldsymbol{R}_{f,h} = \boldsymbol{I}_{f,h} + MO - \mu_f \tag{1}$$

where $\boldsymbol{R}_{f,h}$ and $\boldsymbol{I}_{f,h}$ represent the power of the original ionogram as input and the eliminated ionogram as output, respectively. The subscript f and h indicate the positions of the frequency and altitude values on the ionogram. MO represents the mode value of signal intensity histogram. μ_f is the average of signal intensity at each frequency bin.

As shown in Fig. 1, it is possible to separate the ionospheric echoes and the background noise by estimating the boundary value between them. However, the distribution of signal intensity is different each ionogram. This suggests that it is necessary to estimate the threshold value according to the signal distribution of each ionogram. We estimate this threshold of boundary between the ionospheric echoes and the background noise by ridge regression [8].

Ridge regression is a method which further improves generalization performance by adding an L2 regularization term to multiple regression analysis. For each raw ionogram, Ridge regression estimates the coefficients, w, of multiple regression models for the boundary threshold value as the objective variable, y, and when you give the frequency, mean and variance of the mode of the signal intensity as the explanatory variable, X. The loss function of the ridge regression, L, is shown in Eq. (2), where the weight of the L2 regularization term is $\alpha = 0.7$.

$$L = (y - Xw)^T(y - Xw) + \alpha\|w\|_2^2 \tag{2}$$

$$\hat{y} = X^T w \tag{3}$$

The equation for the objective variable is given by Eq. (3). The above equation yields a model for estimating the threshold for removing an appropriate low-intensity signal. The ionogram after applying this algorithm is shown in Fig. 2.

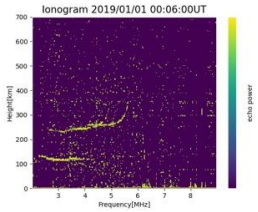

Fig. 2. Ionogram with Weak Signal Reduction applied to Fig. 1a

3.2. *Penalized Background Subtraction*

As shown in Fig. 2, it is still impossible to completely remove the noise from the ionogram, even after removing the low intensity signal. This is because the noise signal is more intense than the ionospheric echoes. We use Background Subtraction method [9] to extract of the ionospheric echoes from the ionogram and to ignore the remained intense background noise. The Background Subtraction method is one of the motion detection techniques to detect moving objects in a video frame. A moving object is detected by comparing a frame of video with its corresponding background image. It is important to generate a background image without moving objects. In this study, we consider an ionospheric echo as the moving object and an ionogram image with only noise present as the background image. The processing part of Penalized Background Subtraction is divided into four steps and the following subsections describe the detail algorithms.

3.2.1. *Penalty based on ionospheric echo shape*

As shown in Fig. 1b, ionospheric echoes in the ionogram are observed mainly as line shapes extending in the frequency direction. This suggests that the signal intensity of ionospheric echoes is higher at specific altitudes than at other altitudes in each frequency band bin. In fact, as shown in Fig. 3b, the distribution of signal intensity against the altitude in interest frequency bin, 4.0 MHz, shows two significant peaks corresponding to the ionospheric echoes.

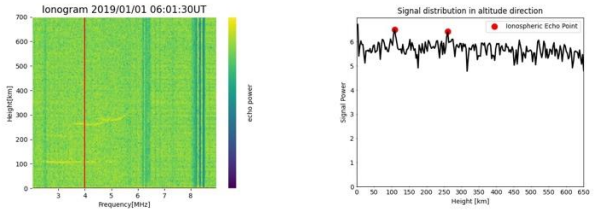

a. Original Ionogram data and the interest frequency, 4.0 MHz, in red vertical line

b. Signal intensity as a function of the altitude for the interest frequency, 4.0 MHz

Fig. 3. Signal distribution in altitude direction, recorded at 06:01:30 UT, January 1, 2019

For generating the background image from the input ionogram image including the ionospheric echoes, we only penalize the corresponded frequency into the significant ionospheric echoes in each ionogram, to reduce the amplitude of signal power. The detail operating flow is as shown in Fig. 4. First, a vector of the signal intensity is extracted for each frequency bin from the two-dimensional matrix of the ionogram. Next, the components that penalize the extracted vectors are selected according to the flowchart shown in the Fig. 4.

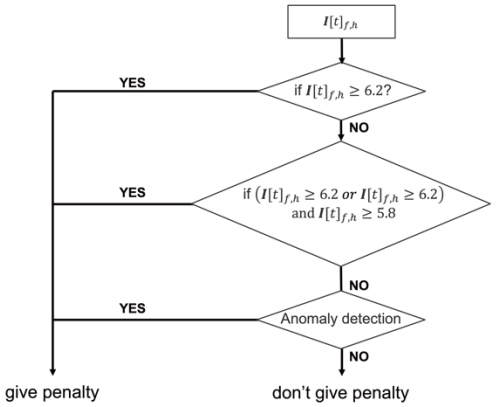

Fig. 4. Determination flow of penalization for the generation of background image

The penalty, $f^{p}_{f,h}$, is given as Eq. (4), where $\boldsymbol{I}[t]_{f,h}$ is the signal intensity of the unprocessed ionogram array at time t. We use anomaly detection in deciding whether to penalize. This is designed based on the Hotelling's theory [10]. In the present work, a normal distribution is assumed for each signal with the same frequency value after removing weak intensity signals, and signals that deviate from the 95% confidence interval are penalized by detecting them as anomalies. By penalizing with these procedures, we ideally aim to get the background image contains only noise.

$$f^{p}_{f,h}(\boldsymbol{I}[t]_{f,h}) = \begin{cases} \dfrac{1}{\boldsymbol{I}[t]_{f,h}} & (penalized) \\ \boldsymbol{I}[t]_{f,h} & (\text{else}) \end{cases} \tag{4}$$

3.2.2. *Penalty based on one previous detection frame image*

The background subtraction method can efficiently detect moving objects under the constraint that the background scene is stationary. However, the accuracy decreases under dynamically changing background image. Ionograms are no exception to this problem, as the position and shape of background noise as well as ionospheric echoes change from moment to moment. Therefore, the ionospheric echoes detected from the previous ionogram are used to estimate the background image.

This method assumes a two-dimensional Gaussian distribution centered on the detected component. Here, the frequency value is f and the height value is h, from which the mean μ_f, μ_h, and standard deviations σ_f and σ_h are calculated, respectively. The covariance ρ is given by Eq. (5), considering the characteristic that the ionospheric echoes vary in the frequency direction. Eq. (6) and (7) show the weight Gaussian. The generated background image is penalized by considering the previous ionospheric echo detection region.

$$\rho = \begin{pmatrix} 8 & 0 \\ 0 & 4 \end{pmatrix} \tag{5}$$

$$f^{g}_{f,h} = \frac{1}{2\pi\sigma_f\sigma_h\sqrt{1-\rho^2}} e^{\alpha} \tag{6}$$

$$\alpha = -\frac{1}{2(1-\rho^2)}\left\{\frac{(f-\mu_f)^2}{{\sigma_f}^2} - \frac{2\rho(f-\mu_f)(h-\mu_h)}{\sigma_f\sigma_h} + \frac{(h-\mu_h)^2}{{\sigma_h}^2}\right\} \tag{7}$$

3.2.3. *Penalized background image generation algorithm*

In addition to the background image update algorithm for the Background Subtraction method [9], the background image, $\boldsymbol{B}[t]$,is updated by adding the weight terms of Eq. (4) and Eq. (6) as follows.

$$\boldsymbol{B}[t] = \alpha \cdot \boldsymbol{B}[t-1] + (1-\alpha) \cdot f^{p}_{f,h}(\boldsymbol{I}[t]) \\ -\beta \cdot f^{g}_{f,h}(\boldsymbol{F}[t-1]) \quad (8)$$

where α and β are weights for $f^{p}_{f,h}$ and $f^{g}_{f,h}$. In this study, we set $\alpha = 0.5$ and $\beta = 8.0$,which are assumed the same level of influence of each term.

3.2.4. *Detection region determination*

The positions where the result of subtracting the background image obtained by Eq. (8) from the input image is a positive value is detected as ionospheric echoes, $\boldsymbol{D}[t]_{f,h}$, as shown in Eq. (9). It is assumed that background regions are distributed where the difference values are small. Thus, $thresh$ in Eq. (9) is set to the class value of the mode in the histogram of difference values between the input and background images.

$$\boldsymbol{D}[t]_{f,h} = \begin{cases} 1 & (\boldsymbol{I}[t]_{f,h} - \boldsymbol{B}[t]_{f,h} \geq thresh) \\ 0 & (else) \end{cases} \quad (9)$$

Fig. 5 shows that our method can detect ionospheric echoes. This indicates that our method is also effective for ionograms with high signal-to-noise ratios.

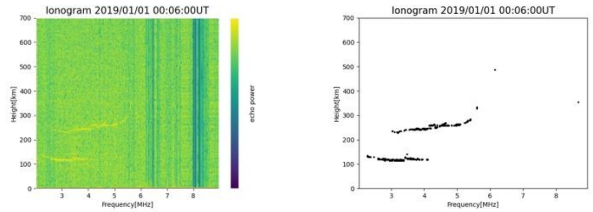

a. Original Ionogram b. Ionogram detection data after processing for Fig. 2

Fig. 5. Ionospheric echo detection by Penalized Background Subtraction, original ionogram data recorded at 00:06:00UT, January 1, 2019

3.3. *Fine-tuning Ionogram*

As shown in Fig. 6a, the background subtraction method can be used to detect ionospheric echoes, but it can also leave isolated noises. In addition, the signal should be detected might have missing or incorrectly detected as the ionospheric echo. For solving these problems, we propose two post-processing methods: the convolution operation to remove noise that appears as isolated echoes, and the optimization for interpolating and denoising of the detection region using an algorithm based on a minimum spanning tree.

3.3.1. *Denoise impulse noise*

The convolution is, an algorithm of image processing, used to reduce of impulse noises in the present work. The multiplication a two-dimensional square matrix composed of odd-numbered widths several times is applied to the detected ionogram with two-dimensional array. If there are many signals around the element of interest that have been labeled as ionospheric echoes by the background subtraction method, then they should be ionospheric echoes, otherwise they should be considered as noise.

The filter $H_{i,j}$ consists of an $n \times n$ square matrix, with all elements 1. It is also scanned with stride 1 to maintain the size of the two-dimensional array of the ionogram. The convolution equation using this filter is shown in Eq. (9). Let D^{bs} be the array output by the algorithm in the processing part of Penalized Background Subtraction and D be the array after impulse noise removal.

$$D_{f,h} = \begin{cases} 1 & \left(\sum_{i=-n}^{n} \sum_{j=-n}^{n} D^{bs}_{f+i,h+j} \cdot H_{i,j} \geq 2 + n \right) \\ 0 & (else) \end{cases} \quad (10)$$

In this study, impulse noises are removed by performing the convolution operation, changing the filter width n in the order of 5, 7, 9, and 11. Ionograms before and after the removal of impulse noises are shown in Fig. 6. It is obvious that this process reduces extracted excess noises and does not disappear the detected signal of ionospheric echoes (Fig. 6b).

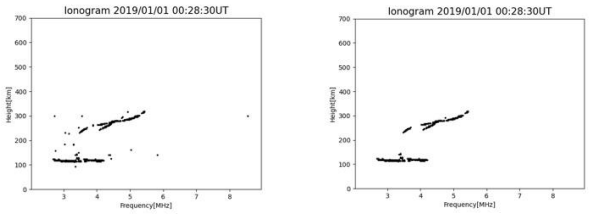

a. Ionospheric echo detection results before processing b. Ionospheric echo detection results after processing

Fig. 6. Comparison of ionograms with and without Impulse noise reduction processing

3.3.2. *Optimization by a minimum spanning tree*

First, for all points detected as ionospheric echoes, these detection points are connected for each E and F layer. The points are connected so that they form a minimum spanning tree, considering the linear shape of the ionospheric echoes. Next, edges with large distances between vertices are removed. The graph to which the removed vertices belong is judged to be noise and removed. For the remained edges after the above processes, the detection area is interpolated between the two vertices that compose the edge. The result is shown in Fig. 7.

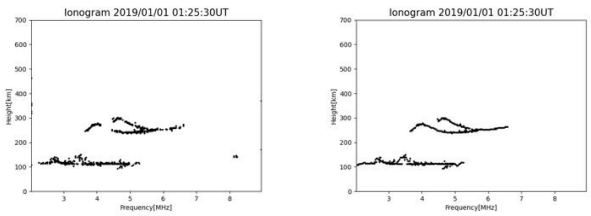

a. Ionospheric echo detection results before processing

b. Ionospheric echo detection results after processing

Fig. 7. Comparison of ionograms with and without optimization process by minimum spanning tree

4. Result and discussion

To evaluate the accuracy of our automatic scaling method, we compared the accuracy of ionograms obtained by our algorithm with that of manually scaled ionograms. The evaluation is based on the absolute error of the critical frequencies' foE and foF of each layer of the ionogram and the percentage of absolute error within 0.5 MHz indicating that sufficient accuracy was achieved. The accuracy of the proposed method is compared with that of the Weighted Background Subtraction without each weight term (Table 1). The average processing time of the proposed algorithm was 7.1 seconds per ionogram. The proposed model successfully reproduces fine ionograms with 98% recall and 99% precision.

Table 1 shows that the detection results were satisfactory despite the low SNR of the ionograms. From Table 1 and the detection result shown in Fig. 7b, it is clearly found that the addition of a weight term to the background subtraction algorithm was effective. The processing time with few of seconds indicates that the proposed method is useful to generate quasi-real-time ionograms with high SNR.

Table 1. Performance Comparison with different weight terms in this study

Model		Main result	Base+ $f_{penalty}$	Base+ f_{gauss}	Base
Absolute error (MHz)	foE	0.47	0.93	0.92	0.99
	foF	0.26	0.44	0.42	2.6
Rate of accuracy (%)	foE	67%	50%	50%	47%
	foF	83%	49%	61%	15%

On the other hand, the continuity of ionospheric echoes remains an issue. Some ionospheric echoes are missing from the detection results of our method. This is due to the altitudinally banded intermodulation noise in the ionograms. This is a factor that reduces the signal strength, and thus causes the background subtraction method to fail to detect the ionospheric echoes. Also, although not present in this study's data set, scattered signals such as those seen in equatorial spread F are not expected to give meaningful results.

5. Conclusion

Automatic scaling of ionograms presents various challenges for the ionogram image contaminated with noises. In this study, we proposed an algorithm to automatically extract ionospheric echoes from ionograms with low signal-to-noise ratio.

Our algorithm is based on statistical thresholding according to the signal intensity distribution of each ionogram, image processing techniques focusing on time variability and ionospheric echo characteristics, noise reduction filtering, and graph theory. Although it is necessary to define some parameters, it is possible to extract ionospheric echoes from ionograms in quasi-real-time without the huge amount of teacher data as in deep learning.

On the other hand, for frequent noise and special ionospheric echo classes, the algorithm may not guarantee accuracy. The algorithm should be improved to be robust in these cases as well for the future work.

Acknowledgements

This work was supported in part by JSPS KAKENHI Grant Numbers JP21K03646, JP21H04518, JP20H01961, JP22K21345.

References

1. B. Zolesi, L. R. Cander, "Ionospheric Prediction and Forecasting", Springer, 2014
2. Z. Chen, S. Wang, S. Zhang, G. Fang, J. Wang, "Automatic scaling of F layer from ionograms", Radio Science, Vol. 48, No. 3, pp. 334–343, 2013.
3. Z. Chen, Z. Gong, F. Zhang, G. Fang, "A new ionogram automatic scaling method", Radio Science, Vol. 53, No. 9, pp. 1149–1164, 2018.
4. C. De La Jara, C. Olivares, "Ionospheric echo detection in digital ionograms using convolutional neural networks", Radio Science, Vol. 56, No. 8, 2021.
5. Z. Xiao, J. Wang, J. Li, B. Zhao, L. Hu, L. Liu, "Deep-learning for ionogram automatic scaling", Advances in Space Research, Vol. 66, No. 4, pp. 942–950, 2020.
6. F. Arıkan, O. Arıkan, S. Salous, "A new algorithm for high-quality ionogram generation and analysis", Radio Science, Vol. 37, No. 1, pp. 1-11, 2002.
7. M. D. E. Turley, A. J. Heitmann, R. S. Gardiner-Garden, "Ionogram RFI Rejection Using an Autoregressive Interpolation Process", Radio Science, Vol. 54, No. 1, pp. 135–150, 2019.
8. D. E. Hilt, D. W. Seegrist, "Ridge: a computer program for calculating ridge regression estimates", Research Note NE-236. Upper Darby, PA: U.S. Department of Agriculture, Forest Service, Northeastern Forest Experiment Station, pp. 1-7, 1977.

9. R. Cutler and L. Davis, "View-based detection and analysis of periodic motion", Proceedings. Fourteenth International Conference on Pattern Recognition (Cat. No.98EX170), Brisbane, QLD, Australia, Vol. 1, pp. 495-500, 1998.
10. H. Hotelling, "Multivariate Quality Control Illustrated by Air Testing of Sample Bombsights", In: Eisenhart, C., Hastay, M.W. and Wallis, W.A., Eds., Techniques of Statistical Analysis, McGraw Hill, New York, pp. 111-184, 1947.

Authors Introduction

Mr. Yuu Hiroshige

He received his Bachelor's degree in Computer Science and Systems Engineering in 2022 from the Faculty of Computer Science and Systems Engineering, Kyushu Institute of technology in Japan. He is currently a master student in Kyushu Institute of Technology, Japan.

Dr. Akiko Fujimoto

She is an Associate Professor at the Faculty of Computer Science and Systems Engineering at Kyushu Institute of Technology in Japan. She graduated from the Department of Earth and Planetary Sciences, Kyushu University, in 2005. She received her Ph.D. degree in Science from Kyushu University in 2010. Her research interest is Space Weather and Upper Atmospheric Sciences.

Dr. Akihiro Ikeda

He is an Associate Professor of the Department of Liberal Arts and Sciences at National Institute of Technology, Kagoshima College in Japan. He graduated from the Department of Earth System Science, Fukuoka University, in 2005. He received his Ph.D. degree in Science from Kyushu University in 2010. His research interest is Upper Atmospheric Sciences.

Dr. Shuji Abe

He is a Research Fellow at the International Research Center for Space and Planetary Environmental Science, Kyushu University in Japan. He graduated from the Department of Earth and Planetary Sciences, Kyushu University, in 1999. He received his Ph.D. degree in Science from Kyushu University in 2005. His research interest is space weather.

Dr. Akimasa Yoshikawa

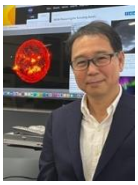

He is a Professor at the Faculty of Sciences, Kyushu University in Japan. He graduated from the Department of Physics, Yamaguchi University, in 1989. He received his Ph.D. degree in Science from Kyushu University in 1998. His research interest is space plasma physics.